Analytical determination of reflection-peak wavelengths of chirped sampled fiber Bragg gratings

Xiaojun Zhu,[1,2] Yuling Lu,[1,2] Guiju Zhang,[1,2] Chinhua Wang,[1,2,*] and Minfu Zhao[1,2]

[1]Key Lab of Modern Optical Technologies of Jiangsu Province, Suzhou, Jiangsu, China

[2]Institute of Modern Optical Technologies, Suzhou University, Suzhou, Jiangsu, 215006, China

*Corresponding author: chinhua.wang@suda.edu.cn

Received 3 December 2007; accepted 9 January 2008;
posted 18 January 2008 (Doc. ID 90398); published 10 March 2008

An analytical expression for calculating the position of the reflection-peak wavelength of a chirped sampled fiber Bragg grating (C-SFBG) is obtained for what is believed to be the first time. Using Fourier theory, the chirped sampling function of the C-SFBG is expanded, and an equivalent local Bragg period is then obtained to derive the expression of the peak wavelength. The calculated results based on the expression are in excellent agreement with the numerical reflection spectra obtained by the conventional transfer-matrix method. © 2008 Optical Society of America

OCIS codes: 060.3735, 050.1590, 060.2310.

1. Introduction

Fiber gratings are essential components in optical communication and fiber sensing systems. Sampled fiber Bragg gratings (SFBGs) have been the subject of considerable interest as potential enabling technologies for applications in multiwavelength filtering [1–3], multichannel dispersion compensation [4–6], optical code-division multiple access [7], etc. A SFBG differs from a standard fiber Bragg grating in that the amplitude or phase or both of the periodic refractive-index change are further modulated by a sampling function (usually a square-wave function). The wavelength separation between channels of a uniform SFBG (U-SFBG) is solely determined by the sampling period owing to the origin of the Fourier transform of the sampling function. The central wavelength position (zeroth order of the Fourier transform) of the U-SFBG is determined by the grating period, and all other reflection-peak positions are derived from the central wavelength position and the wavelength separation between channels. Very recently, an analytical expression for calculating any arbitrary reflection-peak wavelength of the U-SFBG was achieved [8]. The wavelength position of any reflection peak in a U-SFBG can be calculated based on the corresponding Fourier order and the structural parameters of the U-SFBG, which provides an analytical tool for the accurate prediction of the multichannel wavelength position. With the increasing applications of SFBGs, various SFBG structures evolved from U-SFBGs have been proposed and investigated. One typical evolution of such structures is the introduction of chirp into the grating and the sampling function. The various chirping functions in grating period or in sampling function or in combination of both periods provide great flexibility in the design of functional wavelength-division-multiplexed devices. Indeed, there have been several demonstrations of multichannel dispersion compensation (including dispersion slope compensation) in which specific combinations of sampling functions, grating chirps, and interleaved structures were used [4,5]. The general characteristics of the SFBGs that have chirp in the grating period, in the sampling function, or in both have been numerically studied (see [9]), and the features in the spectral and group-delay (dispersion) responses were explained. It was found that the multichannel reflection peaks shift from the corresponding U-SFBG when either the grating period or the sampling function or both

0003-6935/08/081135-06$15.00/0

is chirped. The amount of the shift was obtained numerically using the transfer-matrix (T-matrix) calculation. In view of the importance of the accurate prediction or determination of the wavelength shift (and subsequently, the precise wavelength position of each channel) due to the chirp introduced in the grating parameters, there is a need to develop an analytical rather than a numerical tool to characterize the channel wavelength.

In this paper, we present an analytical expression for the SFBG with a chirp in sampling function. The relationship among the wavelengths of each channel, the chirp coefficient of the sampling function, and the length of the grating is explicitly given. Specifically, the chirped sampling function is first expanded into a new function using Fourier theory, and the equivalent local Bragg period is then obtained to derive the expression of the reflection peak wavelength. The calculated results based on the analytical expression are examined with the conventional numerical results, which are found to be in excellent agreement. This analytical tool can provide insight into the designs of more-complex sampled grating structures and into ways to tailor the parameters properly to obtain a specific performance.

2. Analytical Expression

A SFBG consists of many discrete Bragg grating sections that are separated by nongrating sections periodically. Figure 1 shows typical SFBGs: Fig. 1(a) is a U-SFBG, i.e., the sampling function is uniform in period, and Fig. 1(b) is a chirped sampled fiber Bragg grating (C-SFBG), i.e., the sampling period is linearly chirped along the fiber direction (z axis) with relation

$$b(i) = b_0[1 + (i - 1)c_s], \tag{1}$$

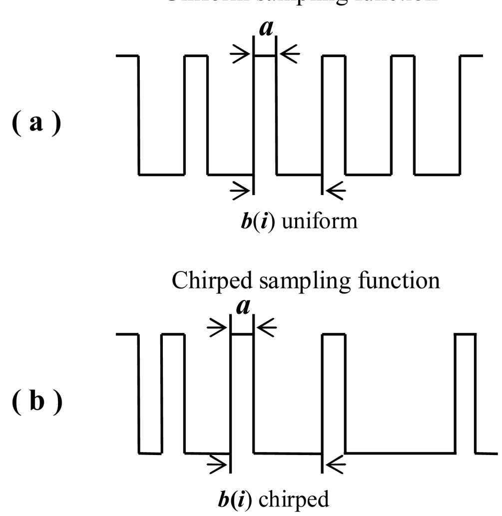

Fig. 1. Configurations of sampled fiber Bragg gratings: (a) Uniform sampled fiber Bragg grating (U-SFBG), (b) chirped sampled fiber Bragg grating (C-FBG), where b is the sampling period and a is the grating length in one period, and $(b - a)$ is the nongrating length.

where $b(i)$ is the ith sampling period, $i = 1, 2 \ldots N$ denotes the sample number, and N is the total number of samples. b_0 is the initial period, and c_s is the linear chirp coefficient of the sampling period. In a C-SFBG (grating period is uniform) with refractive-index modulation distribution $\Delta n(z)$ and sampling function (square wave) $s(z)$ along the z axis, we have the following relations:

$$\Delta n(z) = \Delta n_0 s(z) \mathrm{Re}\left[\exp\left(j\frac{2\pi}{\Lambda_0}\right)\right], \tag{2}$$

$$s(z) = rect\left(\frac{z}{a}\right) * \sum_{m=-\infty}^{+\infty} \delta\left\{z - mb_0\left[1 + \frac{(m-1)}{2}c_s\right]\right\}, \tag{3}$$

where Δn_0 is the peak refractive-index modulation and Λ_0 is the nominal grating period; a is the grating length in each sampling period and remains constant for all of the sampling period, $rect(z/a)$ is the rectangular function, $\delta(x)$ is the delta function, $*$ represents the operator of convolution, and m is an integer ($m = 0, 1, 2 \ldots$). In view of the fact that the term $b_0[1 + (m - 1) \times c_s/2]$ in Eq. (3) is actually the average period of the total m sampling period and c_s is usually very small ($\sim 10^{-3}$–10^{-4}), this term can be considered as a constant p and replaced by the average period of the total N sampling period, assumed in our case to be $p = b_0[1 + (N - 1) \times c_s/2]$. Based on the properties of the delta function, $\delta(x)$, and the Fourier theory, another expression can be derived from Eq. (3):

$$s(z) = \sum_{k=-\infty}^{+\infty} F_k \exp(2\pi jkz/p), \tag{4}$$

where F_k is the Fourier coefficient. Using Eq. (4), Eq. (2) can further be written as

$$\Delta n(z) = \Delta n_0 \sum_{k=-\infty}^{+\infty} F_k \exp\left[2\pi j\left(\frac{1}{\Lambda(k)}\right)z\right], \tag{5}$$

where $\Lambda(k)$ denotes the local Bragg period corresponding to the kth-order Fourier component:

$$\Lambda(k) = \frac{p\Lambda_0}{p - k\Lambda_0}. \tag{6}$$

When k is equal to zero, the value of $\Lambda(0)$ is Λ_0. The reflection-peak wavelengths (RPWs) of C-SFBGs are directly analogous to uniform Bragg gratings as follows:

$$\lambda_{\max}(k) = 2n_0\Lambda(k). \tag{7}$$

Substituting Eq. (6) into (7), the RPWs of each Fourier order (k) of a C-SFBG can be explicitly obtained:

$$\lambda_{\max}(k) = 2n_0 \cdot \frac{b_0\Lambda_0[2+(N-1)c_s]}{b_0[2+(N-1)c_s]-2k\Lambda_0}. \qquad (8)$$

Expression (8) gives the analytical expression of RPWs of C-SFBGs, where n_0 is the effective refractive index in the grating. It is easily seen that when the chirped coefficient $c_s = 0$, the expression reduces to the case of a U-SFBG [8]. As expected, for a U-SFBG, the RPWs of each Fourier order are determined solely by the sampling period and the grating period. The RPWs of a C-SFBG, however, are also a function of the total number of the sampling period (the total length of the grating) in addition to those in the case of a U-SFBG. Using Eq. (8), the deviation of RPWs corresponding to each Fourier order between a C-SFBG and a U-SFBG can also be obtained:

$$\Delta\lambda(k) = 2n_0\left[\frac{k\Lambda_0^2(b_0-p)}{(b_0-k\Lambda_0)(p-k\Lambda_0)}\right], \qquad (9)$$

where b_0 is the initial period of the C-SFBG and also the sampling period of the U-SFBG. From Eq. (9), it is seen that (a) when the total number of sampling period N is fixed and the chirp coefficient $c_s > 0$, (i.e., $p > b_0$), the deviation $\Delta\lambda(k)$ is negative, which means the high-order Fourier reflection peaks will shift towards the zeroth-order (central) peak. However, when the chirp coefficient $c_s < 0$, (i.e., $p < b_0$), the deviation $\Delta\lambda(k)$ is positive, which means high-order Fourier reflection peaks will shift away from the zeroth-order (central) peak. (b) When the chirp coefficient c_s is fixed and the total number of sampling N is increased, the deviation of RPWs will shift towards the zeroth-order peak while the RPWs will shift away from the zeroth order when the total number of samples N is decreased.

3. Simulation Results and Discussions

In order to confirm the analytical expression obtained above, we use the numerical T-matrix technique to directly calculate the reflection-peak wavelengths and compare the results with those obtained by the analytical expression. We first compare the spectral features between U-SFBGs and C-SFBGs numerically by using the T-matrix method. In the simulations, we assume that $n_0 = 1.485$ (the effective refractive index), $\Lambda_0 = 521.8855\,\text{nm}$ (central wavelength $\lambda = 1550\,\text{nm}$), $\Delta n_0 = 6.0 \times 10^{-4}$, and $N = 30$ (the number of sampling periods). Figure 2 shows the wavelength shift of the corresponding reflection peaks between a U-SFBG ($c_s = 0$) and C-SFBG with a different chirp coefficient c_s. Figure 2(a) shows the wavelength shift in the full wavelength range, while Fig. 2(b) shows the enlarged details of the wavelength shift over three channels of Fig. 2(a). In the calculation, $b_0 = 1\,\text{mm}$ (the first period) and $a = 0.08\,\text{mm}$ (a is fixed for all of the sampling period) are assumed. To view the effect of the chirp coefficient on the wavelength shift, three different c_s are used: $c_s = 0$ (U-SFBG), $c_s = 7 \times 10^{-4}$, and $c_s = 1.5 \times 10^{-4}$. It is shown in Fig. 2 that the wavelength of the central reflection peak (zeroth Fourier order) does not shift with varying c_s. All high-order reflection peaks (both positive and negative Fourier orders), however, shift toward (or away from) the zeroth-order peak (i.e., central reflection peak) when c_s is positive (or negative). The wavelength shift is positively correlated with the chirp coefficient and the Fourier order. The higher the Fourier order, the larger the wavelength shift, and the larger the chirp coefficient, the larger the wavelength shift.

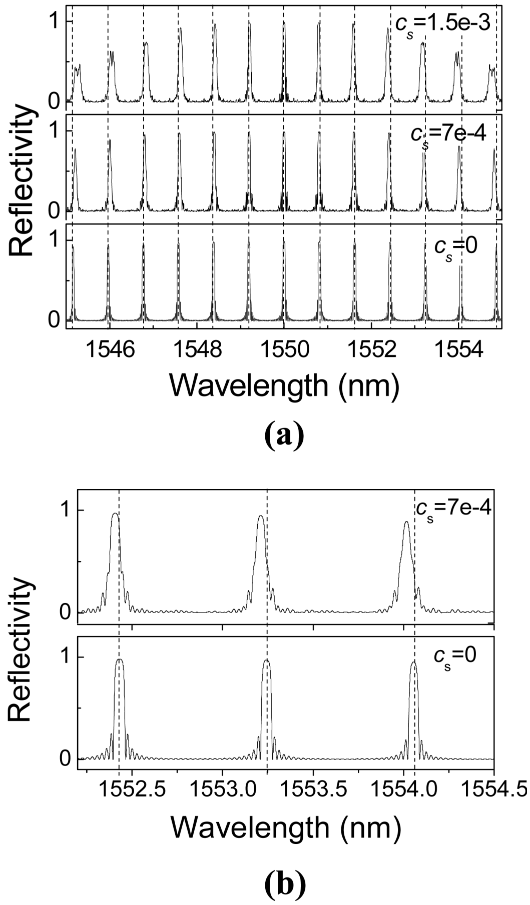

Fig. 2. (a) Wavelength shift of the corresponding reflection peaks between a U-SFBG ($c_s = 0$) and C-SFBG with different chirp coefficient c_s. In the calculation, $b_0 = 1\,\text{mm}$ (the first period) and $a = 0.08\,\text{mm}$ (a is fixed for all of the sampling period) are assumed, and three different c_s are used: $c_s = 0$ (U-SFBG), $c_s = 70 \times 10^{-4}$, and $c_s = 1.5 \times 10^{-3}$. (b) Enlarged details of the wavelength shift over three channels of Fig. 2(a).

We now focus our attention on the detailed numerical values of the wavelength shift of each Fourier order and the comparison of the RPWs between numerical value (calculated by T-matrix technique) and analytical value [calculated by the analytical expression of Eq. (8)]. Table 1 shows the analytically and numerically calculated RPWs of three different chirp coefficient c_s based on Eq. (8) and the T-matrix method. In the calculation, the following parameters are used: the initial period $b_0 = 1\,\text{mm}$, the grating length in each sampling period $a = 0.08\,\text{mm}$ (fixed), total number of the sampling period $N = 30$, $n_0 = 1.485$, the central wavelength is set at $\lambda = 1550\,\text{nm}$

Table 1. Calculated RPWs of Three Different Chirp Coefficients c_s Based on Analytical Expression and the T-Matrix Method

Chirp Coefficient		RPWs of Different Fourier Order (nm) with Different c_s								
		−4	−3	−2	−1	0	1	2	3	4
Uniform ($c_s = 0$)	Numerical	1546.769	1547.574	1548.386	1549.191	1550	1550.809	1551.621	1552.434	1553.246
	Analytical	1546.771	1547.577	1548.384	1549.192	1550	1550.809	1551.620	1552.431	1553.242
$c_s = 1.5 \times 10^{-3}$	Numerical	1546.836	1547.626	1548.416	1549.206	1550	1550.788	1551.584	1552.380	1553.171
	Analytical	1546.840	1547.629	1548.418	1549.209	1550	1550.792	1551.585	1552.379	1553.173
$c_s = 3 \times 10^{-3}$	Numerical	1546.897	1547.671	1548.447	1549.221	1550	1550.779	1551.554	1552.329	1553.111
	Analytical	1546.905	1547.678	1548.451	1549.225	1550	1550.776	1551.552	1552.329	1553.107

(corresponding grating period $\Lambda_0 = 521.8855\,\text{nm}$), and the chirp coefficients c_s are assumed to be 0, 1.5×10^{-3}, and 3×10^{-3}, respectively. From Table 1, it is clear that the detailed wavelength positions of the corresponding Fourier orders can be quantitatively obtained with the derived analytical expression, and the results obtained with the analytical and numerical methods are in excellent agreement. Figure 3 shows the comparison of the results obtained with analytical and numerical methods graphically. In Fig. 3, the numerical results (num) are plotted with different lines, and the analytical results (ana) with different symbols. We see from Fig. 3 that (1) different chirp coefficients introduce different wavelength shifts; the larger c_s, the larger the shift. In the case of positive chirp coefficient c_s (as the case in Fig. 3), the wavelength shifts toward the central wavelength (1550 nm) of the zeroth order, and (2) for the same c_s, different Fourier orders have different shifts. The higher the order, the larger the shift. Figure 4 shows the detailed deviations between the analytical and the numerical results for different Fourier orders. The typical deviation between the numerical and the analytical results is about 0.008 nm, which is very close to the step size (which was set at 0.004 nm) in our numerical calculation. Detailed examination shows that the deviation between the analytical and the numerical results is mainly from the error in determining the RPWs in the numerical method in which the wavelength uncertainty around the peak point (one calculating point before or after the peak) is about 0.008 nm (more or less the same as the typical deviation). If the step size was reduced to 0.002 nm, the deviation between the analytical and the numerical was found to be ~0.004 nm, which further confirms the consistency between the analytical and the numerical methods.

To further show the capability of the developed analytical tool in predicting the RPWs for the C-SFBG, Fig. 5 gives the comparison between the analytical and numerical results with a chirp coefficient of $c_s = 1.5 \times 10^{-3}$ for sampling periods, $b_0 = 1, 2$, and 3 mm. The initial duty cycle (a/b_0) is fixed at 0.08 for the three different sampling periods. Other parameters are the same as those used in Fig. 3. As expected, with different sampling periods, the channel spacing varies, as witnessed by the different slopes in Fig. 5. Again, it is seen that the deviations between the analytical and numerical results for all three different sampling periods are very small (~0.008 nm) and mainly from the error in numerical determination of wavelength of the reflection peak. The comparison indicates that the analytical expression is highly accurate in predicting analytically the RPW for arbitrary C-SFBGs.

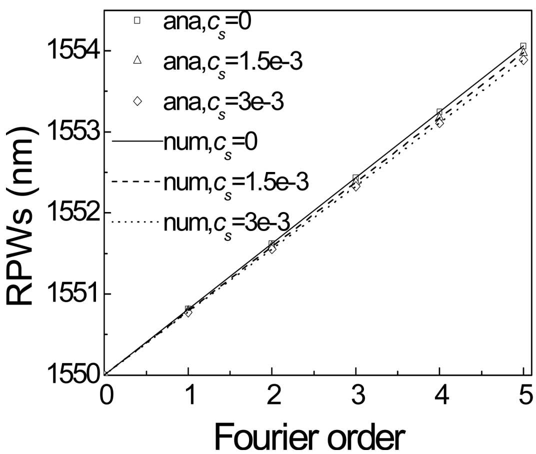

Fig. 3. Comparison of the RPWs results obtained with analytical and numerical methods for three different chirp coefficients: $c_s = 0$ (U-SFBG), $c_s = 1.5 \times 10^{-3}$, and $c_s = 3 \times 10^{-3}$. Lines, numerical; symbols, analytical.

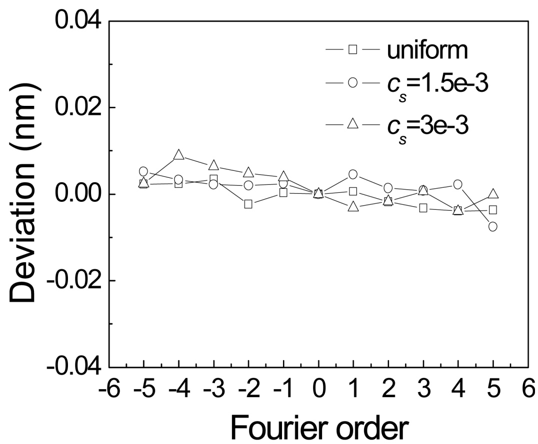

Fig. 4. Relative deviations between the analytical and the numerical results for different Fourier orders with different chirp coefficients. $c_s = 0$ (squares), $c_s = 1.5 \times 10^{-3}$ (circles), and $c_s = 3 \times 10^{-3}$ (triangles).

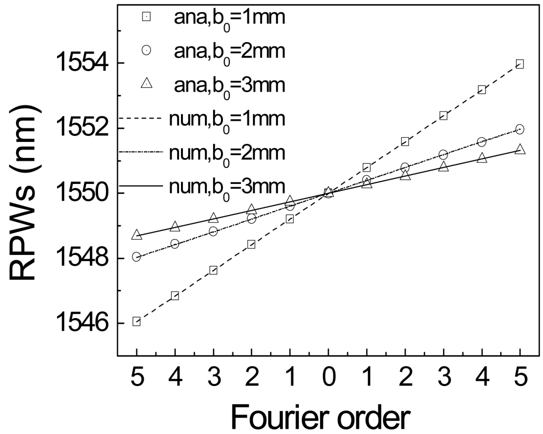

Fig. 5. Comparison between the analytical and numerical results with a chirp coefficient of $c_s = 1.5 \times 10^{-3}$ for different sampling periods, $b_0 = 1\,\text{mm}$ (squares), $b_0 = 2\,\text{mm}$ (circles), and $b_0 = 3\,\text{mm}$ (triangles). All numerical results are plotted with lines.

As mentioned in Eq. (8), the RPWs of a C-SFBG are also a function of the number of the sampling period N in addition to the chirp coefficient c_s and other grating parameters. This is an important feature of C-SFBGs and is different from that of a U-SFBG, in which the RPWs are independent of the number of the sampling period, i.e., the total length of the grating. Using Eq. (8), we can also predict the RPWs of the C-SFBGs with arbitrary length, for which otherwise we must resort to complicated numerical calculations. Figure 6 shows the wavelength shift of the corresponding reflection peaks with different total number of sampling periods N ($N = 10$, 25, and 40). In the calculation, $b_0 = 1\,\text{mm}$ (the first period), $a = 0.08\,\text{mm}$ (a is fixed for all the sampling period), and $c_s = 1.5 \times 10^{-3}$ are assumed. As shown in Fig. 6, the wavelength shift increases with increasing N at fixed c_s. The detailed comparison between the numerical results and the analytical results obtained using Eq. (8) for chirp coefficient $c_s = 3 \times 10^{-3}$ are shown in Fig. 7 (the other parameters are the same as those used in Fig. 6), which exhibits again excellent agreement between the numerical and the analytical results.

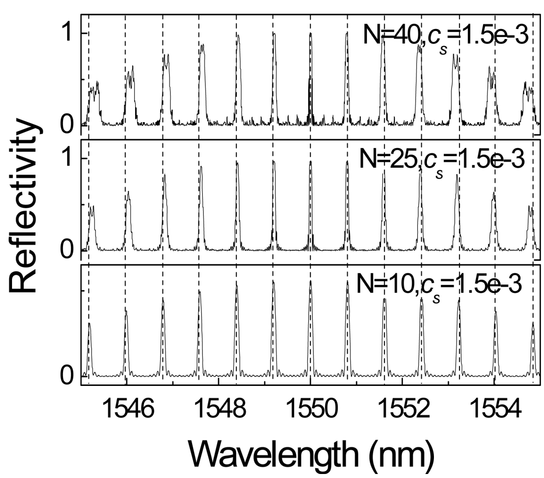

Fig. 6. Wavelength shift of the corresponding reflection peaks with different total number of sampling periods N (= 10, 25, and 40). In the calculation, $b_0 = 1\,\text{mm}$ (the first period), $a = 0.08\,\text{mm}$ (a is fixed for all the sampling period), and $c_s = 1.5 \times 10^{-3}$.

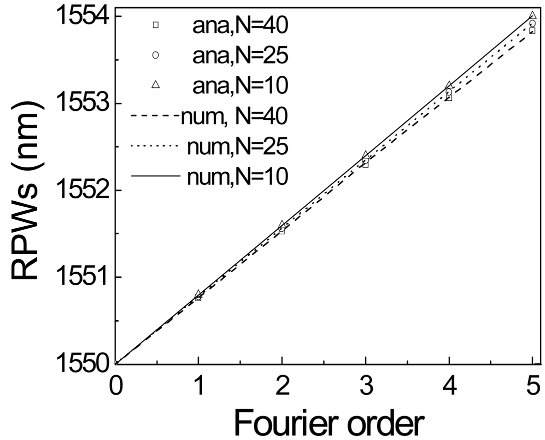

Fig. 7. Comparison of the RPWs results obtained with analytical and numerical methods for three different total number of sampling periods N (= 10, 25, and 40). The chirp coefficient $c_s = 3 \times 10^{-3}$, and the other parameters are the same as those used in Fig. 6. Numerical results (num), lines; analytical results (ana), symbols.

4. Conclusions

We expand the analytical expression of U-SFBGs to arbitary C-SFBGs based on Fourier theory. In the expression, the chirp coefficient, the sampling period, the total length of the grating, and the corresponding Fourier orders are involved to calculate RPWs for different wavelength channels. The analytically calculated results are in excellent agreement with the numerically obtained results. The analytical expression provides a highly accurate tool in predicting the RPWs for arbitrary C-SFBGs with an arbitrary number of sampling periods, which includes U-SFBGs when the chirp coefficient is equal to zero. It is expected that the obtained analytical formula will be useful in the design and the characterization of complex SFBG structures.

Support through research funds from Suzhou University (Contract No. Q4108612) is gratefully acknowledged.

References

1. M. Ibsen, M. K. Durkin, M. J. Cole, and R. I. Laming, "Sinc-sampled fiber Bragg gratings for identical multiple wavelength operation," IEEE Photon. Technol. Lett. **10**, 842–844 (1998).
2. C. Wang, J. Azaña, and L. R. Chen, "Efficient technique for increasing the channel density in multiwavelength sampled fiber Bragg grating filters," IEEE Photon. Technol. Lett. **16**, 1867–1869 (2004).
3. N. Yusuke and Y. Shinji, "Densification of sampled fiber Bragg gratings using multiple phase shift (MPS) technique," J. Lightwave Technol. **23**, 1808–1817 (2005).

4. W. H. Loh, F. Q. Zhou, and J. J. Pan, “Sampled fiber grating based-dispersion slope compensator,” IEEE Photon. Technol. Lett. **11**, 1280–1282 (1999).
5. F. Ouellette, P. A. Krug, T. Stephens, G. Dhosi, and B. Eggleton, “Broadband and WDM dispersion compensation using chirped sampled fiber Bragg gratings,” Electron. Lett. **11**, 899–901 (1995).
6. X.-F. Chen, Y. Luo, C.-C. Fan, T. Wu, and S.-Z. Xie, “Analytical expression of sampled Bragg gratings with chirp in the sampling period and its application in dispersion management design in a WDM system,” IEEE Photon. Technol. Lett. **12**, 1013–1015 (2000).
7. M. S. Kumar and A. Bekal, “Performance evaluation of SSFBG based optical CDMA systems employing golden sequences,” Opt. Fiber Technol. **11**, 56–68 (2005).
8. X. H. Zou, W. Pan, B. Luo, W. L. Zhang, and M. Y. Wang, “Accurate analytical expression for reflection-peak wavelengths of sampled Bragg grating,” IEEE Photon. Technol. Lett. **18**, 529–531 (2006).
9. C. H. Wang, L. R. Chen, and P. W. E. Smith, “Analysis of chirped-sampled and sampled-chirped fiber Bragg gratings,” Appl. Opt. **41**, 1654–1660 (2002).